

## Theory of one-dimensional hopping conductivity and diffusion\*

Peter M. Richards

Sandia Laboratories, Albuquerque, New Mexico 87115

(Received 6 April 1977)

Hopping motion is considered in a linear chain containing an arbitrary density of particles that are not allowed to hop to occupied sites. The general case of two inequivalent lattice sites  $A$  and  $B$  is treated. Transition-rate equations are solved by Monte Carlo simulation and, where possible, by analytic techniques. Only for the case of equivalent sites do the results here agree with those recently obtained by Huber from nonlinear differential equations for site occupancy which neglect certain correlations. The conductivity is mean-field-like for equivalent sites, but shows sizeable departure for inequivalent sites, having an activation energy increased over the mean-field value. Here "mean-field" behavior is one where the only effect of forbidden hops to occupied sites is to reduce effective transition rates by a factor  $1 - n$ , where  $n$  is the average occupation number of the site to which a jump occurs. The velocity correlation function is shown to consist of a  $\delta$ -function part which reproduces the mean-field conductivity and a function  $\beta(t)$  which is negative for times  $t > 0$ . This is qualitatively quite different from the picture given by Huber's equations. Motion of a single distinguishable particle shows an anomalous  $x^2 \propto t^{1/2}$  dependence of the mean square displacement upon time  $t$ , but the displacement  $X$  of all the particles does obey a diffusion relation  $X^2 \propto t$ . This difference is explained in terms of the number of particles which have to be pushed aside in order for a particle to move a distance  $x$ , and in terms of the ensuing density fluctuation. Differences between time dependences and attempt frequencies as measured by bulk conductivity and microscopic probes such as NMR are noted and discussed in light of data on the one-dimensional superionic conductor  $\beta$  eucryptite ( $\text{LiAlSiO}_4$ ). Reinterpretation of NMR relaxation data on some of the organic charge-transfer salts is also suggested.

### I. INTRODUCTION

Quasi-one-dimensional (1D) conductivity is manifested in a variety of physical systems under present investigation. Among these are superionic conductors such as  $\beta$ -eucryptite ( $\text{LiAlSiO}_4$ ) for which fast ion motion takes place dominantly along 1D channels and organic conductors and/or semiconductors like tetrathiafulvalene-tetracyanoquinodimethane (TTF-TCNQ) which display highly anisotropic conductivity.<sup>2</sup> In the localized-state limit associated with ionic conductivity or with short-mean-free-path electronic motion it may be appropriate to describe the dynamics by nearest-neighbor hopping.

For noninteracting particles such hopping equations give rise to single-particle diffusion expressed by

$$x_\alpha^2 = 2D_s t, \quad (1)$$

where  $x_\alpha^2$  is the mean-square displacement of a distinguishable particle in time  $t$ , and  $D_s$  is the single-particle diffusion coefficient. The conductivity  $\sigma$  in the same model is

$$\sigma = N_v e^2 D / k_B T \quad (2)$$

for  $N_v$  carriers per unit volume of charge  $e$  at temperature  $T$ , as follows from the Einstein-Nernst formula.<sup>3</sup> Here  $D$  is the bulk diffusion coefficient and is equal to  $D_s$  for noninteracting particles.

When the particles interact through Coulomb re-

pulsion the situation is much more complicated, even in a classical hopping model such as considered here. A common practice is to assume that the repulsion is sufficiently strong to forbid two or more particles from occupying the same lattice site but to neglect nearest-neighbor and longer-range repulsions. Thus the particles are taken as noninteracting except for an exclusion principle which allows hops to unoccupied sites only. This approach, used in the present paper, is obviously an oversimplification but it has the advantage of treating the dominant effect of repulsion so that it may not differ qualitatively from a hopping model in which finite-range interactions are also included.

The simplest approximation is one in which the rate for hopping to a site  $j$  is reduced by the factor  $1 - n_j$ , where  $n_j$  is the thermal equilibrium probability that site  $j$  is occupied. (For two types of sites  $A$  and  $B$ ,  $n_j$  has the value  $n_A$  or  $n_B$ .) The hopping equations are then linear just as in the noninteracting case and the only effect is to reduce  $D_s$ , and thereby  $\sigma$ , by the same factor. We refer to this as a mean-field calculation, and a major object of the paper is to investigate the extent to which mean-field theory is applicable.

Mean-field theory breaks down completely for single-particle "diffusion." Instead of (1) we find the relation

$$x_\alpha^2 \propto t^{1/2}, \quad (3)$$

so that diffusion in the normal sense does not ex-

ist. Not only is the above unpredictable by mean-field theory, it is also indescribable by a correlation factor<sup>4</sup> which is commonly used for diffusion in two and three dimensions (2D and 3D). It is found, however, that the total displacement  $X = \sum_{\alpha} x_{\alpha}$  of all the particles is diffusive,

$$X^2 = 2N_p Dt \quad (4)$$

for  $N_p$  particles and that the relation (2) holds. Thus bulk properties such as conductivity and single-particle motion as obtained by microscopic probes such as NMR<sup>5</sup> are not related in a simple way, and this can have an appreciable effect on the interpretation of experimental data, as is discussed later.

The results of Eqs. (3) and (4) and others to be presented were obtained by Monte Carlo simulations of the hopping motion on closed chains (periodic boundary conditions) containing typically 4000 particles and 8000 available sites. It has in some cases been possible to give analytical derivations of the results and/or present physical arguments which justify them. In particular we establish the consistency of Eqs. (3) and (4) in terms of the strong 1D correlations and give expressions for the conductivity in terms of the relevant parameters.

Huber<sup>6</sup> has recently treated the same 1D system with infinite on-site repulsion in terms of nonlinear differential equations for the probability of site occupancy. This approach has at least three drawbacks compared with a Monte Carlo or purely stochastic computation. First, since the equations are only for site occupancy, they are incapable of describing distinguishable particle motion and therefore miss important features such as Eq. (3). Second, they give a velocity correlation function  $\langle V(t)V(0) \rangle$ , where  $V$  is the total velocity of all particles, which is identically zero for all  $t$ , including  $t=0$ , in an infinite system with all lattice sites equivalent. One cannot, therefore, reliably calculate the conductivity in this framework by the standard Kubo formalism<sup>7</sup>

$$\sigma \propto \int_0^{\infty} \langle V(t)V(0) \rangle dt. \quad (5)$$

We are able to show that the Monte Carlo equations yield

$$\langle V(t)V(0) \rangle = \alpha \delta(t) \quad (6)$$

for equivalent sites and thereby resolve the difficulty. Third, the nonlinear differential equations give different results from the Monte Carlo ones for long-time behavior of the site occupancy. This discrepancy can be important in, for example, low-frequency NMR studies which can sample the long-time decay of site occupancy. Reasons for the difference, which occurs only if there are inequi-

valent sites, are discussed. The two methods do give the same results for site occupancy when all sites are equivalent since in this case the *site* equations become linear.<sup>6</sup>

As in Ref. 6 we consider a lattice with two sites per unit cell  $A$  and  $B$  which in general are inequivalent. The following results for the conductivity are derived analytically and confirmed by the Monte Carlo. Let  $W_{AB}$  and  $W_{BA}$  be the transition rates for hopping from  $A$  to  $B$  and from  $B$  to  $A$ , respectively. If the sites are equivalent,  $W_{AB} = W_{BA}$ , the only effect of exclusion of hops to occupied sites is to reduce  $\sigma$  by a factor  $1 - n_A = 1 - n_B$  from its non-interacting-particle value so that mean-field theory works in this special case. This is connected with the fact that the velocity correlation is zero for unequal times as pointed out in Eq. (6). If the sites are inequivalent, however, such that  $W_{AB} \ll W_{BA}$ , then a novel result is obtained: whereas mean field gives  $\sigma \propto W_{AB}$ , more accurate analysis predicts a further reduction so that  $\sigma \propto W_{AB}(W_{AB}/W_{BA})^{1/2}$  for  $\rho = \frac{1}{2}$  ( $\rho$  is the average number of particles per site). Thus, if  $\Delta_A$  and  $\Delta_B$  are the barriers for jumping from the deep  $A$  and shallow  $B$  sites, respectively, the activation energy is increased from  $\Delta_A$  to  $\Delta_A + \frac{1}{2}(\Delta_A - \Delta_B)$ . The correction is shown to arise from the  $t \neq 0$  contribution of  $\langle V(t)V(0) \rangle$  to the integral in Eq. (5). The  $\delta$ -function part (6) yields the mean-field conductivity.

The paper is organized as follows. Section II presents the hopping equations as used in a Monte Carlo calculation and points out the similarities and differences with the nonlinear rate equations of Ref. 6. The thermal-equilibrium properties are derived in Sec. III. The conductivity is calculated in Sec. IV A by finding the net velocity in an applied field, while its computation by the Kubo formula (5) is discussed in Sec. IV B. Single-particle and bulk diffusion are examined in Sec. V. The results are summarized and discussed in Sec. VI with particular emphasis placed on the relation between conductivity and Raman-scattering data in  $\beta$ -eucryptite and interpretation of NMR experiments in TCNQ salts. Details of the Monte Carlo calculation are presented in an Appendix.

## II. HOPPING EQUATIONS

In this section we write equations for the hopping process as calculated by Monte Carlo methods and compare them with the nonlinear differential equations in Ref. 6. The more-complex equation (7) is introduced rather than starting with the standard form, Eq. (10), so that we may properly treat the velocity correlation later.

The model consists of a chain of even number  $N$  sites at positions  $x_i = an_i$  ( $n_i = 0, 1, 2, \dots, N$ ) con-

taining  $\rho N$  particles. Odd-numbered sites are *A*-type and even numbered ones are *B*-type. The stochastic Monte Carlo hopping equations for the change  $\delta P_i$  are

$$\begin{aligned} \delta P_i = & -\eta(i, i+1)P_i(1-P_{i+1})P_{i-1} \\ & -\eta(i, i-1)P_i(1-P_{i-1})P_{i+1} \\ & -\eta'(i, i\pm 1)P_i(1-P_{i\pm 1})(1-P_{i-1}) \\ & +\eta(i+1, i)(1-P_i)(1-P_{i-1})P_{i+1} \\ & +\eta(i-1, i)(1-P_i)(1-P_{i+1})P_{i-1} \\ & +\eta'(i\pm 1, i)(1-P_i)P_{i\pm 1}P_{i-1}. \end{aligned} \quad (7)$$

Here  $P_j$  has the value of 1 if site  $j$  is occupied and 0 if it is unoccupied. The quantities  $\eta$  and  $\eta'$  are variables which have the value 0 or 1 according to a random number  $R$  as follows. The number  $R$  has a square distribution between 0 and 1. We introduce a number  $p_{ij}$  such that if  $0 \leq R(i, j) \leq p_{ij}$ ,  $\eta(i, j) = 1$ , and  $\eta(i, j) = 0$  if  $R(i, j) > p_{ij}$ . The indices  $(i, j)$  on  $R$  and  $\eta$  indicate that each possible transition  $i \rightarrow j$  entails a separate call to the random number generator. It is evident that

$$\bar{\eta}(i, j) = p_{ij}, \quad (8)$$

where the bar indicates an average over many values of  $R$ , and thus  $p_{ij}$  represents the probability of hopping from  $i$  to  $j$ . The quantity  $\eta'(i, j)$  is defined such that it is equal to 1 if  $0 \leq R(i, j) \leq 2p_{ij}$  and zero otherwise, so

$$\bar{\eta}'(i, j) = 2p_{ij}. \quad (9)$$

Validity of Eqs. (8) and (9) requires  $p_{ij} \leq 0.5$  since  $0 \leq R \leq 1$ . The probabilities  $p_{ij}$  are restricted to  $j = i \pm 1$  and have values  $p_{AB}$  or  $p_{BA}$  for  $i$ , an *A* site or a *B* site, respectively, in the absence of an applied electric field.

The sense of Eq. (7) is as follows. First note that only one of the six terms on the right-hand side can be nonzero. For example, if sites  $i$  and  $i+1$  are occupied and  $i-1$  is unoccupied, then only the second term on the right-hand side survives. This is because the exclusion effect is included and of course a hop cannot occur out of site  $i$  unless there is a particle there to begin with. The nonzero term on the right-hand side represents the one possibility for a hop to take place, in the present example from  $i$  to  $i-1$ . If the "throw of the dice" (call to  $R$ ) produces  $\eta = 1$ , the hop occurs; otherwise there is no hop. Note also that the change  $\delta P_i$  can only assume the values 0,  $\pm 1$ .

The third and sixth terms on the right-hand side require special attention. If the third term is nonzero, a hop can occur to either of two vacant sites; and the probability for this is just the sum of the probabilities for the single hops. Hence  $\bar{\eta}'(i, i \pm 1)$

$= p_{i, i+1} + p_{i, i-1}$  for  $p_{i, i \pm 1} \ll 1$ , which we assume throughout. Likewise, a nonzero sixth term means that either of two particles can jump into the vacant site, which leads to  $\bar{\eta}'(i \pm 1, i) = p_{i+1, i} + p_{i-1, i}$  for  $p_{i \pm 1, i} \ll 1$ . Questions as to how one decides to which one of two vacant sites a particle jumps or which one of two particles jumps into a vacant site are discussed in the Appendix which contains a more-detailed description of the Monte Carlo calculation. Periodic boundary conditions are imposed by taking  $i+1 = 1$  for  $i = N$  and  $i-1 = N$  for  $i = 1$ .

The Monte Carlo calculation proceeds by examining each site  $i$  and changing occupations as prescribed by Eq. (7). After all  $N$  sites have been treated the steps are repeated with the new occupation numbers  $P_i + \delta P_i$ . Each time the process is carried through the full  $i = 1$  to  $N$  cycle we say that the time  $t$  increases by an amount  $\delta t$ . The calculation of a quantity over  $n$  Monte Carlo cycles (for time up to  $t = n\delta t$ ) is repeated a large number of times, with different random numbers at each step, to obtain a statistical average.

To transform (7) to a differential equation we perform an average over many Monte Carlo cycles so that the  $\eta$ 's are replaced by their average values whereby

$$\begin{aligned} \delta \bar{P}_i^* = & -p_{i, i+1}P_i(1-P_{i+1}) - p_{i, i-1}P_i(1-P_{i-1}) \\ & + p_{i+1, i}(1-P_i)P_{i+1} + p_{i-1, i}(1-P_i)P_{i-1}. \end{aligned} \quad (10)$$

Here  $\delta \bar{P}_i^*$  represents the average change of  $P_i$  for a given value of the occupation numbers  $P_i, P_{i \pm 1}$ . That is, the average leading from (7) to (10) is taken only over the  $\eta$ 's with the  $P$ 's fixed. Note that the terms involving a product of three  $P$ 's cancel when this average is taken so that Eq. (10) has the standard form of a rate equation with hops to occupied sites excluded. A further average must be taken, however, before time development can be described. This is evident from the fact that  $\delta \bar{P}_i^*$  can be no larger than  $p_{i+1, i} + p_{i-1, i}$ , whereas  $P_i, P_{i \pm 1}$  on the right-hand side are still restricted to be 1 or 0. Thus we do not yet have  $P_i(t + \delta t) = P_i(t) + \delta \bar{P}_i^*$ . To accomplish this a further average must be taken over all the different values of  $P_i(t)$  which have resulted from applying many Monte Carlo cycles starting from the same initial condition. Not only do we average over the  $\eta$ 's for the Monte Carlo cycle at  $t$ , we average over all past  $\eta$ 's which leads to an average distribution at  $t$ . This additional average is denoted by a bar over the right-hand side of (12), and it then follows that

$$\bar{P}_i(t + \delta t) = \bar{P}_i(t) + \delta \bar{P}_i = \bar{P}_i(t) + \delta t \frac{d\bar{P}_i}{dt}, \quad (11)$$

with the second equality holding for sufficiently small values of  $p_{ij}$ . The differential equation is

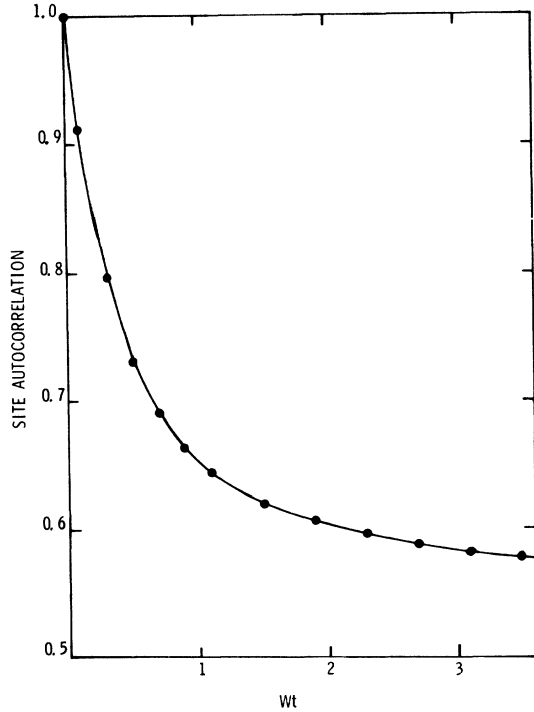


FIG. 1. Normalized site autocorrelation function  $\langle P_{iA}(t)P_{iA}(0) \rangle / P_{iA}(0)^2$  for equivalent sites  $W_{AB} = W_{BA} = W$ . Circles are Monte Carlo results ( $Wt = pn$ , where  $n$  is the number of Monte Carlo steps) for  $p = 10^{-2}$ , 4000 particles on 8000 sites, average over 40 different thermal-equilibrium initial conditions. Curve is analytical result given in Ref. 6.

then

$$\frac{d\bar{P}_i}{dt} = -W_{i,i+1}(\bar{P}_i - \bar{P}_{i+1}) - W_{i,i-1}(\bar{P}_i - \bar{P}_{i-1}) + W_{i+1,i}(\bar{P}_{i+1} - \bar{P}_{i,i+1}) + W_{i-1,i}(\bar{P}_{i-1} - \bar{P}_{i,i-1}) \quad (12)$$

where  $W_{ij} = p_{ij}/\delta t$  and where  $P_{i,j} = P_i P_j$  describes joint occupation of sites  $i$  and  $j$ .

Since they will be used frequently, we summarize the notations for three kinds of averages. For a quantity  $Q$ ,  $\bar{Q}^*$  is an average only over the present random variables  $\eta$  which occur explicitly in the equation for the change in occupations at a particular time, as in Eq. (7);  $\bar{Q}$  is an average over all past  $\eta$ 's which occur implicitly as a result of the time development from a fixed initial condition, as in Eq. (10). The thermal average  $\langle Q \rangle = \langle \bar{Q} \rangle$  contains an additional averaging over many initial configurations of the  $P_i$  subject to the thermal equilibrium conditions given in Sec. III.

The quantity  $\bar{P}_i$  is interpreted as the probability that site  $i$  is occupied and is a continuous variable in Eq. (12). Similarly  $\bar{P}_{i,i+1}$  is the probability for simultaneous occupancy of  $i$  and  $i \pm 1$ . The approximation of Ref. 6 was to let

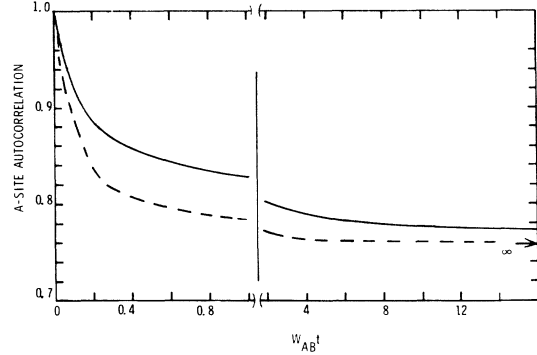


FIG. 2. Normalized  $A$ -site autocorrelation function for inequivalent sites  $W_{AB} = 0.1 W_{BA}$ . Solid curve is Monte Carlo result for  $p_{AB} = 0.1 p_{BA} = 10^{-2}$ , 4000 particles on 8000 sites, average over 40 different thermal-equilibrium initial conditions. Dashed curve is numerical result obtained in Ref. 6.

$$\bar{P}_{i,i+1} = \bar{P}_i \bar{P}_{i+1} \quad (13)$$

and thereby neglect any correlations. In general, Eq. (13) is not valid so that differences between the Monte Carlo results presented here and those of Ref. 6 can result. A special case is for equivalent sites in the absence of a field ( $W_{i,i\pm 1} = W_{i\pm 1,i} = W$ ). Then, as noted by Huber, the  $\bar{P}_{i,i\pm 1}$  terms cancel so that the site equations are linear.

The difference between the two methods for inequivalent sites and equality for equivalent sites is illustrated in Figs. 1 and 2. The quantity shown is the normalized  $A$ -site thermal-equilibrium autocorrelation function<sup>8</sup>  $\langle P_{iA}(t)P_{iA}(0) \rangle$  for  $W_{AB} = W_{BA}$  and  $W_{AB} = 0.1 W_{BA}$ . Correspondence between the number of Monte Carlo cycles  $n$  and the time variable  $t$  is achieved through the relation  $p_{AB} n = W_{AB} t$ . The  $t \rightarrow \infty$  value of  $\langle P_{iA}(t)P_{iA}(0) \rangle$  is assumed to be  $\langle P_{iA} \rangle^2$  and given by considerations of Sec. III.

### III. THERMAL-EQUILIBRIUM PROPERTIES

Thermal-equilibrium properties are of importance for the inequivalent site problem and are discussed in this section, both in terms of the hopping equations and a model Hamiltonian for classical particles which obey an exclusion principle but are otherwise noninteracting.

The steady-state solution to (12) is

$$W_{AB} n_A (1 - n_B) = W_{BA} n_B (1 - n_A) \quad (14)$$

in the absence of a field ( $W_{iA,iA\pm 1} = W_{AB}$ ,  $W_{iA\pm 1,iA} = W_{BA}$ ), where  $n_A(n_B) = \langle \bar{P}_i \rangle$  for  $i$  an  $A(B)$  site and the thermal probabilities are assumed to be uncorrelated [Eq. (13)]. Lack of correlation may be justified by representing the system by the Hamiltonian

$$\mathcal{H} = - \sum_{i=1}^N \Delta_i n_i, \quad (15)$$

where  $\Delta_i = \Delta_A$  ( $\Delta_B$ ) for  $i$  odd (even) and  $n_i$  is a number operator which can assume only the values 1 or 0. We then find by usual methods of the grand canonical ensemble

$$n_A = \{1 + \exp[-(\Delta_A + \mu)/k_B T]\}^{-1}, \quad (16)$$

$$n_B = \{1 + \exp[-(\Delta_B + \mu)/k_B T]\}^{-1}, \quad (17)$$

and

$$\begin{aligned} \langle n_i n_{i+1} \rangle &= \exp[(\Delta_A + \Delta_B + 2\mu)/k_B T] \\ &\times \{1 + \exp[(\Delta_A + \mu)/k_B T] \\ &\quad + \exp[(\Delta_B + \mu)/k_B T] \\ &\quad + \exp[(\Delta_A + \Delta_B + 2\mu)/k_B T]\}^{-1} \\ &= n_A n_B. \end{aligned} \quad (18)$$

Equations (16) and (18) are consistent with the detailed balance condition

$$W_{BA}/W_{AB} = \exp[(\Delta_A - \Delta_B)/k_B T].$$

The condition  $n_A + n_B = 2\rho$  fixes the chemical potential  $\mu$  and allows determination of  $n_A$  and  $n_B$ . For a half-filled lattice  $2\rho = 1$ , we see that (14) reduces to

$$\frac{n_A}{n_B} = \left(\frac{W_{BA}}{W_{AB}}\right)^{1/2} = \exp[(\Delta_A - \Delta_B)/2k_B T]. \quad (19)$$

Although there is no correlation in thermal equilibrium in zero field, steady-state correlations do appear when a field is applied, as shall be demonstrated.

#### IV. CONDUCTIVITY

The conductivity may be calculated in two ways from the hopping equations. First there is the same method an experimentalist would use: Apply a field and measure the ensuing current. If a weak field  $E$  is applied in the  $+x$  direction, the barrier for hopping is changed by an amount  $\pm \frac{1}{2}eEa$ , where the upper (lower) sign is for hops to the right (left). (Any effects of higher order than linear in  $E$ , such as shifting of the positions of the potential minima and maxima, are ignored throughout.) We assume positive ions so that the charge  $e$  is positive. For thermally activated hopping over a barrier we then have

$$W_{i_A, i_{A+1}} = W_{AB} \exp(\pm \Delta) \approx W_{AB} (1 \pm \Delta), \quad (20)$$

where

$$\Delta = eEa/2k_B T \quad (21)$$

and  $\Delta \ll 1$  has been assumed. A similar equation holds for  $W_{i_B, i_{B+1}}$ .

The current density is given by

$$J = e\Omega^{-1}V_E, \quad (22)$$

where  $V_E$  is the net steady-state drift velocity of all the particles in a field and  $\Omega$  is the volume per particle ( $\Omega$  is the unit-cell volume for equivalent sites).

The net Monte Carlo velocity  $V_{MC}(n)$  of all the particles is defined as the number of hops to the right minus the number of hops to the left which take place at the  $n$ th cycle:

$$\begin{aligned} V_{MC}(n) &= \sum_i \eta_{i, i\pm 1} P_i (1 - P_{i+1}) \\ &\quad - \eta_{i+1, i} P_{i+1} (1 - P_i), \end{aligned} \quad (23)$$

where the  $\eta$ 's and  $P$ 's are evaluated at the Monte Carlo time integer  $n$ . This is readily converted to an average velocity  $\bar{V}$  with proper dimensions by replacing the  $\eta$ 's with their average values  $\bar{\eta}_{i,j} = p_{ij} = W_{ij}/\delta t$  and noting that a Monte Carlo jump corresponds to moving a distance  $\pm a$  in a time  $\delta t$ . Thus

$$\begin{aligned} \bar{V} &= a \sum_i [W_{i, i+1} (\bar{P}_i - \bar{P}_{i+1}) \\ &\quad - W_{i+1, i} (\bar{P}_{i+1} - \bar{P}_{i+1, i})], \end{aligned} \quad (24)$$

and  $V_E$  represents the steady-state value of  $\bar{V}$  in a field. Details of the solution of Eq. (24) will be given in Sec. IV A.

A second method, popular with theorists, is to use the Kubo formula of Eq. (5) repeated here as

$$\sigma = \frac{J}{E} = \frac{e^2}{\Omega k_B T} \int_0^\infty \langle V(t)V(0) \rangle dt, \quad (25)$$

where the thermal equilibrium correlation function is calculated in zero field, so that  $V$  is calculated by (23) with  $\Delta = 0$ .

##### A. Velocity in presence of field

We compute here conductivity by the first method of finding the steady-state velocity in presence of a field. Equation (24) yields

$$\begin{aligned} \bar{V} &= a(W_{BA} - W_{AB}) \sum_{i_A} (\bar{P}_{i_A, i_{A+1}} - \bar{P}_{i_A, i_{A-1}}) \\ &\quad + 2a\Delta(W_{AB}N_A + W_{BA}N_B) \\ &\quad - a\Delta(W_{AB} + W_{BA}) \sum_{i_A} (\bar{P}_{i_A, i_{A+1}} + \bar{P}_{i_A, i_{A-1}}), \end{aligned} \quad (26)$$

after some rearrangement of summation indices and neglecting end effects either by assuming periodic boundary conditions or by letting  $N \rightarrow \infty$ . The summations above are over the odd numbered  $A$  sites, hence the index  $i_A$ , so that  $P_{i_{A+1}}(P_{i_{A-1}})$  is the occupation number for the neighboring  $B$  site to the right (left) of  $i_A$ . The quantities  $N_A$  and  $N_B$  are the total number of particles on  $A$  sites and  $B$  sites, respectively.

In the steady state  $\bar{P}_{i_A, i_{A+1}}$  must be independent of  $i_A$  so that Eq. (26) reduces to

$$V_E = a(W_{BA} - W_{AB})(\frac{1}{2}N)y + 2a\Delta(W_{AB}N_A + N_{BA}N_B) - a\Delta(W_{AB} + W_{BA})N\tau, \quad (27)$$

where we have noted that there are  $\frac{1}{2}NA$  sites and introduced the correlations

$$\tau = \frac{1}{2}(\{\bar{P}_{i_A, i_{A+1}}\} + \{\bar{P}_{i_A, i_{A-1}}\}), \quad (28a)$$

$$y = \{\bar{P}_{i_A, i_{A+1}}\} - \{\bar{P}_{i_A, i_{A-1}}\}, \quad (28b)$$

in which the curly brackets indicate a steady-state average in the presence of a field. Symmetry requires  $y=0$  in zero field or for equivalent sites in an arbitrary field, but  $y$  is not necessarily zero for  $W_{AB} \neq W_{BA}$  and  $\Delta \neq 0$ . In fact we shall show that  $y$  makes an appreciable contribution to the conductivity for inequivalent sites. Steady-state conditions also require  $\{d\bar{P}_i/dt\} = 0$  which from (12), (20), and (28) translate to

$$-2W_{AB}(\bar{n}_A - \tau) + 2W_{BA}(\bar{n}_B - \tau) + \Delta(W_{AB} + W_{BA})y = 0, \quad (29)$$

where  $\bar{n}_A = \{\bar{P}_{i_A}\}$ ,  $\bar{n}_B = \{\bar{P}_{i_{A+1}}\}$  are now the mean occupation numbers in presence of a field. The same equation (29) is obtained by using either  $\{dP_{i_A}/dt\} = 0$  or  $\{dP_{i_B}/dt\} = 0$ .

Consider the solution to lowest order in  $\Delta$ . Since  $\Delta=0$  corresponds to zero field, we have from the results of Sec. III,

$$\bar{n}_A = n_A + O(\Delta), \quad (30a)$$

$$\bar{n}_B = n_B + O(\Delta), \quad (30b)$$

$$\{\bar{P}_{i_A, i_{A+1}}\} = \langle \bar{P}_{i_A, i_{A+1}} \rangle + O(\Delta) = n_A n_B + O(\Delta). \quad (31)$$

Equation (31) implies

$$y = O(\Delta), \quad (32)$$

where  $O(\Delta)$  means of the order of  $\Delta$  or of higher order in  $\Delta$ .

Equations (30)–(32) are inserted in (27) to give

$$V_E = a(W_{BA} - W_{AB})(\frac{1}{2}N)y + Na\Delta[W_{AB}n_A(1 - n_B) + W_{BA}n_B(1 - n_A)] + O(\Delta^2). \quad (33)$$

For  $y=0$  we have the mean-field (MF) or no-correlation result for the velocity

$$V_E(\text{MF}) = Na\Delta[W_{AB}n_A(1 - n_B) + W_{BA}n_B(1 - n_A)] + O(\Delta^2), \quad (34)$$

which gives a  $\Delta \rightarrow 0$  conductivity of

$$\sigma_{\text{MF}} = (Ne^2/\Omega k_B T)a^2 W_{AB}n_A(1 - n_B) \quad (35)$$

from (14), (21), and (22). Note that Eq. (35) is

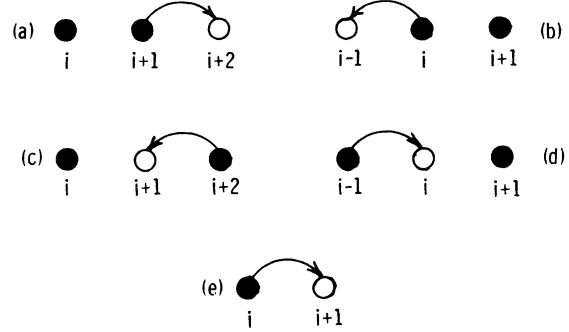


FIG. 3. Diagrams illustrating terms in hopping equations. Solid circles represent occupied sites, open circles unoccupied sites. Arrows indicate direction of hops. (a)–(d) Terms in Eq. (36) for  $(d/dt)\bar{P}_{i, i+1}$ . Diagrams (a)–(d) are in one-to-one correspondence with four terms on right-hand side of (36) with upper sign taken. (e) Term in  $\bar{P}_i(d/dt)\bar{P}_{i+1}$  which contributes to  $(d/dt)(\bar{P}_i\bar{P}_{i+1})$  but not to  $(d/dt)(\bar{P}_{i, i+1})$ .

generally correct,  $\sigma = \sigma_{\text{MF}}$ , for equivalent sites since the coefficient of  $y$  in (33) is proportional to  $W_{BA} - W_{AB}$ .

Since the term in  $y$  of Eq. (29) is  $O(\Delta^2)$ , that equation gives no information regarding  $y$ , at least in our method of considering  $\Delta$  as a small perturbation. To determine  $y$  we write the rate equations for  $d(\bar{P}_{i, i+1})/dt$ ,

$$\begin{aligned} \frac{d}{dt}\bar{P}_{i, i+1} = & -W_{BA}(1 \pm \Delta)(\bar{P}_{i, i+1} - \bar{P}_{i, i+1, i+2}) \\ & - W_{AB}(1 \mp \Delta)(\bar{P}_{i, i+1} - \bar{P}_{i, i+1, i+1}) \\ & + W_{AB}(1 \mp \Delta)(\bar{P}_{i, i+2} - \bar{P}_{i, i+1, i+2}) \\ & + W_{BA}(1 \pm \Delta)(\bar{P}_{i+1, i+1} - \bar{P}_{i, i+1, i+1}), \quad (36) \end{aligned}$$

where  $i$  is an  $A$  site and  $P_{i, j, k}$  is the probability of simultaneous occupation of the three sites  $i, j, k$ . The separate terms in Eq. (36) are shown diagrammatically in Figs. 3(a)–3(d) to display their meaning more clearly. Note that  $d(\bar{P}_{i, i+1})/dt \neq d(\bar{P}_i\bar{P}_{i+1})/dt$  which indicates that correlations do occur which affect the results of Ref. 6. The terms differ by the fact that

$$\frac{d}{dt}(\bar{P}_i\bar{P}_{i+1}) = P_i \frac{d\bar{P}_{i+1}}{dt} + P_{i+1} \frac{d\bar{P}_i}{dt} \quad (37)$$

contains terms shown in Fig. 3(e) such as  $\bar{P}_i W_{AB} \bar{P}_{i+1}(1 - \bar{P}_{i+1})$  which do not contribute to  $d(\bar{P}_{i, i+1})/dt$ . The steady-state condition  $d(\{\bar{P}_{i, i+1}\} - \{\bar{P}_i\bar{P}_{i+1}\})/dt = 0$  gives

$$-(W_{AB} + W_{BA})y + 2\Delta W_{BA}(f_{BB} - f_{BAB} + f_{ABA} - \tau) - 2\Delta W_{AB}(f_{AA} - f_{ABA} + f_{BAB} - \tau) = 0, \quad (38)$$

where the  $f$ 's are new correlations defined by

$$f_{AA} = \{\bar{P}_{i_A, i_{A+2}}\}, \quad (39)$$

$$f_{ABA} = \{\bar{P}_{i_A, i_{A+1}, i_{A+2}}\}, \quad (40)$$

so that  $f_{AA}$  is the correlation between two  $A$  sites separated by a distance  $2a$  and  $f_{ABA}$  is a corresponding three-site correlation. Similar definitions hold for  $f_{BB}$  and  $f_{BAB}$ . Symmetry does require  $\{\bar{P}_{i_A, i_{A+2}}\} = \{\bar{P}_{i_A, i_{A-2}}\} = f_{AA}$ , etc., but it does not require  $\{\bar{P}_{i_A, i_{A+1}}\} = \{\bar{P}_{i_A, i_{A-1}}\}$  if  $W_{AB} \neq W_{BA}$  and  $\Delta \neq 0$ .

A solution for  $y$  valid to first order in  $\Delta$  is obtained by replacing the  $f$ 's and  $\tau$ 's by their  $\Delta=0$  uncorrelated values  $f_{AA} = n_A^2$ ,  $f_{ABA} = n_A^2 n_B$ ,  $\tau = n_A n_B$ , etc., whence

$$y = -4\Delta W_{AB} n_A (1 - n_B)(n_A - n_B) / (W_{AB} + W_{BA}), \quad (41)$$

where we have made use of the equilibrium condition (14). For equivalent sites  $n_A = n_B$  and  $y = 0$  as expected. The result  $y < 0$  for  $W_{BA} > W_{AB}$  ( $n_A > n_B$ ) may be understood as follows. With  $W_{BA} > W_{AB}$ , a particle at an  $A$  site may be thought of as slow moving and one at a  $B$  site as fast moving since current is limited by the  $A \rightarrow B$  hopping rate. The quantity  $y$  then represents the difference in likelihoods of finding a fast moving particle to the right of  $A$  and to the left of  $A$ . For a net drift to the right ( $\Delta > 0$ ) the motion of a  $B$  particle to the left of  $A$  is inhibited on the average whereas there is no such "pile up" to the right. Thus, it is more likely to find a particle to the left of  $A$  than to the right, so  $y < 0$  in this situation. A highway analogy may also be helpful. Traffic jams occur behind slow moving vehicles rather than in front of them.

By using result (41) in (33)–(35), we obtain

$$\sigma = \sigma_{MF} \left( 1 - \frac{W_{BA} - W_{AB}}{W_{BA} + W_{AB}} (n_A - n_B) \right). \quad (42)$$

The correction to the mean-field conductivity  $\sigma_{MF}$  becomes particularly severe for  $\rho \geq \frac{1}{2}$  since then  $n_A \rightarrow 1$  and  $\sigma/\sigma_{MF} \rightarrow 0$  for  $W_{BA} \gg W_{AB}$ . For  $\rho = \frac{1}{2}$  so that  $n_A + n_B = 1$ , Eq. (42) reduces to

$$\sigma = 2\sigma_{MF} n_A n_B / (n_A^2 + n_B^2) \approx 2\sigma_{MF} (W_{AB}/W_{BA})^{1/2} \quad (43)$$

for  $W_{BA} \gg W_{AB}$ . Since  $\sigma_{MF}$  is proportional to  $W_{AB}$  in the same limit, the above shows that the activation energy is increased from the MF value  $\Delta_A$  to  $\Delta_A + \frac{1}{2}(\Delta_A - \Delta_B)$  if one assumes  $W_{AB} \propto \exp(-\Delta_A/k_B T)$  and  $W_{BA} \propto \exp(-\Delta_B/k_B T)$  for phonon-assisted hopping rates with the site barriers  $\Delta_{A,B} \gg k_B T$ .

In Fig. 4 we present evidence from the Monte Carlo calculations in support of Eq. (42) for  $W_{BA} = 10 W_{AB}$  and  $\rho = \frac{1}{2}$ , which gives  $n_A = 0.760$ ,  $n_B = 0.240$ . The Monte Carlo velocity is  $V_{E,MC} = V_E(\delta t/a)$  according to the discussion between Eqs. (23) and (24) and so is obtained from  $V_E$  by replacing  $W_{AB}(W_{BA})$  by the jump probability  $p_{AB}(p_{BA})$  and taking unit hopping distance. The specific calculation has  $p_{AB} = 0.01$ ,  $p_{BA} = 0.1$ , and  $\Delta = 0.1$  for which Eqs. (34) and (42) yield  $V_{E,MC}/\rho N = 2.31 \times 10^{-3}$ ,  $1.33 \times 10^{-3}$  for the mean-field and complete values, respectively, per particle.  $V_{E,MC}/\rho N$  is plotted as a function of the number of Monte Carlo cycles  $n(t = n\delta t)$  in Fig. 4. Initially  $V_{E,MC}$  is close to the mean-field value but it decays to a steady-state level in good agreement with the prediction of Eq. (42). The reason that  $V_{E,MC}$  starts out near the mean-field uncorrelated value is that, as in all Monte Carlo calculations presented here, the initial conditions correspond to thermal equilibrium in the absence of a field so that the correlations which make (42) differ from (34) are initially absent. In other words the plot of  $V_{E,MC}$  vs  $n$  in Fig. 4 is one for which  $\Delta$  is a step function applied at  $n$

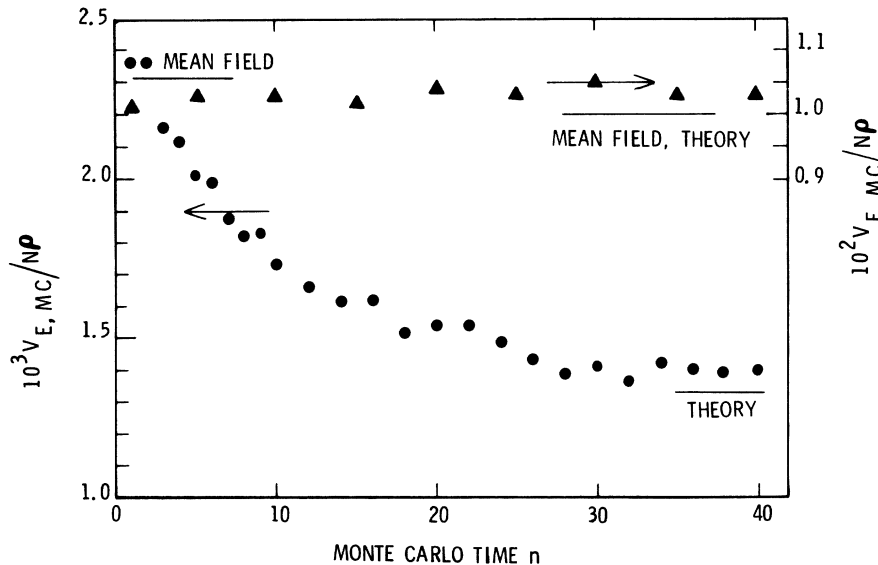


FIG. 4. Average Monte Carlo velocity per particle in a field vs Monte Carlo time integer  $n$ . Circles:  $W_{AB} = 0.1 W_{BA}$  ( $p_{BA} = 0.1$ ,  $p_{AB} = 0.01$ ); triangles:  $W_{AB} = W_{BA}$  ( $p_{AB} = p_{BA} = 0.1$ ). Both sets of data have  $\Delta = 0.1$ ,  $N\rho = 1000$  particles on 2000 sites, average over 20 000 different thermal equilibrium initial conditions. Line labeled "Mean field" is Eq. (34) to first order in  $\Delta$ . Line labeled "Theory" has mean-field value multiplied by correction factor in square brackets of Eq. (42). "Mean Field" = "Theory" for  $W_{AB} = W_{BA}$ .

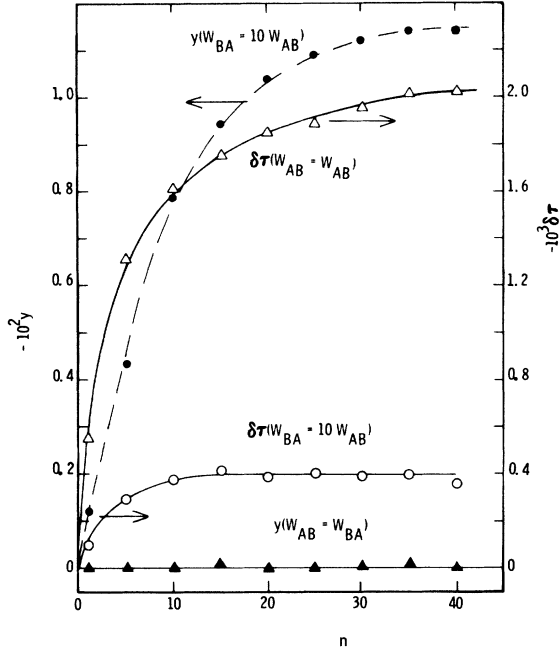


FIG. 5. Correlations  $y$  and  $\delta\tau = \tau - n_A n_B$  in a field vs Monte Carlo time integer  $n$ .  $y$  values are to be read on scale at left,  $\delta\tau$  values on scale at right. Note that, where nonzero, both  $y$  and  $\delta\tau$  are negative. Results are taken from same computer runs used in Fig. 4.

= 0 to a thermal distribution. Figure 5 shows time development of the correlations  $\delta\tau \equiv \tau - n_A n_B$  and  $y$ . Not shown are  $\tilde{n}_A$  and  $\tilde{n}_B$  which maintain the values  $n_A$  and  $n_B$  within statistical error. To first order in  $\Delta$ , Eq. (41) predicts  $y = 1.09 \times 10^{-2}$  in the steady state for parameters used in the  $W_{BA} = 10W_{AB}$  curve. The previous equations are not adequate to give expressions for  $\tilde{n}_A$ ,  $\tilde{n}_B$ , and  $\tau$  beyond their zero-correlation values, but Eq. (29) shows that the combination  $-W_{AB}(\tilde{n}_A - \tau) + W_{BA}(\tilde{n}_B - \tau)$  is of the order of  $\Delta^2$  which is consistent with  $n_{A,B} = n_{A,B} + O(\Delta^2)$ ,  $\tau = n_A n_B + O(\Delta^2)$ , and this appears to agree with the results in Fig. 5.

Figures 4 and 5 also give results for equivalent sites using  $p_{AB} = p_{BA} = 0.1$ ,  $\Delta = 0.1$ . Here we see that  $V_{E,MC}$  has the mean-field value for all times in agreement with  $y = 0$  for equivalent sites. We further note, however, that  $\tau - n_A n_B$  has significantly larger magnitude than for the inequivalent site calculation. For  $W_{AB} = W_{BA}$ , Eq. (29) reduces to  $0 = 0$  so that we cannot make the same inferences as in the above paragraph regarding  $\tau$ .

### B. Velocity correlation

We show here that the zero-field velocity correlation function may be written

$$\langle V(t)V(0) \rangle = \alpha \delta(t) + \beta(t)\Theta(t), \quad (44)$$

where  $\delta(t)$  is the Dirac  $\delta$  function and  $\Theta(t)$  is the step function which is unity for  $t > 0$ . If Eq. (13) were valid,  $\beta(t)$  would be the same as given in Ref. 6 where the velocity correlation was written

$$\langle V(t)V(0) \rangle_{\text{Huber}} = \tilde{\beta}(t), \quad (45)$$

with  $\tilde{\beta}(t)$  calculated assuming in (13) that  $\bar{P}_{i, i\pm 1} = \bar{P}_i \bar{P}_{i\pm 1}$ , and the step function would not be necessary. It is further demonstrated that  $\alpha$  contains the mean-field approximation to the conductivity. That is, upon using the Kubo relation (25), we have

$$\sigma_{\text{MF}} = (e^2 / \Omega k_B T) (\frac{1}{2} \alpha), \quad (46)$$

and thus  $\beta(t)$  makes up the difference

$$\sigma - \sigma_{\text{MF}} = \frac{e^2}{\Omega k_B T} \int_0^\infty \beta(t) dt. \quad (47)$$

To establish the above equations we use the Monte Carlo velocity defined in Eq. (23) in terms of the random variables  $\eta_{i,j}$ . The equal-times correlation contains averages of products of random variables such as  $\langle \eta_{i, i+1} \eta_{j, j+1} \rangle_{\text{av}}$ . These are uncorrelated unless they refer to the same jump and thus, in general,

$$\langle \eta_{i, i'} \eta_{j, j'} \rangle_{\text{av}} = p_{i, i'} p_{j, j'} + (p_{i, i'} - p_{i, i'}^2) \delta_{i, j} \delta_{i', j'}, \quad (48)$$

since  $\eta_{i, i'}$  can only assume the values 0 or 1 ( $\eta_{i, i'}^2 = \eta_{i, i'}$ ) and  $\bar{\eta}_{i, i'} = p_{i, i'}$ . Keeping only the uncorrelated first term or the right-hand side of (48) reproduces Huber's equation

$$\tilde{\beta}(0) = Na^2 (W_{BA} - W_{AB})^2 n_A n_B (1 - n_A) (1 - n_B). \quad (49)$$

However, in the limit of small hopping probability which is assumed throughout, the term in Eq. (48) linear in  $p_{i, i'}$  dominates, and use of this fact in the square of  $V_{\text{MC}}(0)$  leads to

$$\langle V_{\text{MC}}(0)^2 \rangle = N [p_{AB} n_A (1 - n_B) + p_{BA} n_B (1 - n_A)] \quad (50)$$

or

$$\langle V(0)^2 \rangle = (Na^2 / \delta t) [W_{AB} n_A (1 - n_B) + W_{BA} n_B (1 - n_A)], \quad (51)$$

which shows the  $\delta$  function character in the limit of the time interval  $\delta t \rightarrow 0$ . The precise relation is

$$\alpha = 2Na^2 W_{AB} n_A (1 - n_B), \quad (52)$$

which is found by trapezoidal-rule numerical integration with  $\langle V(\delta t)V(0) \rangle \ll \langle V(0)^2 \rangle$  (see below) together with the fact that  $\int_0^\infty \delta(t) dt = \frac{1}{2}$  and we have used the thermal equilibrium condition (14).

Consider now  $\langle V(t)V(0) \rangle$  for  $t = 0+$ , which is proportional to  $\langle V_{\text{MC}}(1)V_{\text{MC}}(0) \rangle$  if we take  $t = 0$  to refer to the first Monte Carlo cycle  $n = 0$  and if we take the limit of vanishingly small hopping probabilities. This correlation function contains terms such as

$$\langle \eta_{i, i+1}(1) \eta_{j, j+1}(0) P_i(1) P_j(0) \rangle_{\text{av}}$$



evaluated at  $n=1$  or 0 as shown. Since there is no correlation between random numbers called at different cycles  $n$  it might at first appear that each  $\eta$  appearing in the above can be replaced by its average value. It is true that the replacement

$$\langle \eta_{i,i+1}(1)\eta_{j,j+1}(0)P_i(1)P_j(0) \rangle_{av} = p_{i,i+1} \langle \eta_{j,j+1}(0)P_i(1)P_j(0) \rangle_{av} \quad (53)$$

can be made (here angular brackets with the subscript "av" indicate an average over the variables  $\eta_i$ , i.e., they have the same meaning as a bar above a quantity), but an important feature is that  $P_i(1) = P_i(0) + \delta P_i(0)$  implicitly contains a random number called at  $n=0$  which is then correlated with  $\eta_{j,j+1}(0)$  for values of  $i$  and  $j$  such that the same  $j \rightarrow j+1$  jump is considered in the equation for  $\delta P_i$ . We then have

$$\langle \eta_{j,j+1}(0)P_i(1)P_j(0) \rangle_{av} = p_{j,j+1} [\bar{P}_{i,j}(0) + \langle \delta P_i(0)P_j(0) \rangle_{av}] + O(p^2), \quad (54)$$

where  $\delta P_i(0)$  contains only that portion of  $\delta P_i(0)$  which involves a  $j \rightarrow j+1$  jump, which of course implies that  $i=j$  ( $i \rightarrow i+1$ ) or  $i=j+1$  ( $i \rightarrow i$ ). For small hopping probabilities we neglect the  $O(p^2)$  term in (54). If  $p_{j,j+1}\bar{P}_{i,j}(0)$  were the only term included, we would find  $\langle V(0+)V(0) \rangle = \bar{\beta}(0+) = \bar{\beta}(0)$  since Huber's  $\bar{\beta}(t)$  is continuous at  $t=0$  and is obtained by replacing the  $\eta$ 's in Eq. (23) by their average values. The correction  $\langle \delta P_i(0)P_j(0) \rangle_{av}$  is significant, however, and we find after some algebra

$$\langle V(0+)V(0) \rangle = \bar{\beta}(0) - 2Na^2(W_{BA} - W_{AB}) \times W_{AB}(n_A - n_B)n_A(1 - n_B) \quad (55)$$

upon using the prescription outlined in the discussion surrounding Eq. (54) in the correlation obtained from Eq. (23). In the above,  $\bar{\beta}(0)$  is as given in Eq. (49) and the second term on the right-hand side represents the  $\langle \delta P_i(0)P_j(0) \rangle_{av}$  correction in (54). Use also has been made of the thermal-equilibrium condition in Eq. (14). Further use of (14) shows that for the half-filled lattice ( $n_A + n_B = 1$ ),

$$Na^2(W_{BA} - W_{AB})W_{AB}(n_A - n_B)n_A(1 - n_B) = Na^2(W_{BA} - W_{AB})^2 n_A^2 n_B^2 = \bar{\beta}(0),$$

so that we obtain the amusing result

$$\langle V(0+)V(0) \rangle = \beta(0+) = -\bar{\beta}(0) \quad (56)$$

for  $\rho = \frac{1}{2}$ . The correlation has the same magnitude as that given in Ref. 6 for  $t \rightarrow 0$  but is of opposite sign.

Since  $\langle V(0+)V(0) \rangle / \langle V(0)^2 \rangle$  is of the order of  $W_{BA}\delta t \ll 1$ , expressions (44) and (52) for the  $\delta$ -function behavior are justified. The contributions of  $\alpha\delta(t)$  and  $\beta(t)$  to the integration are in general of the

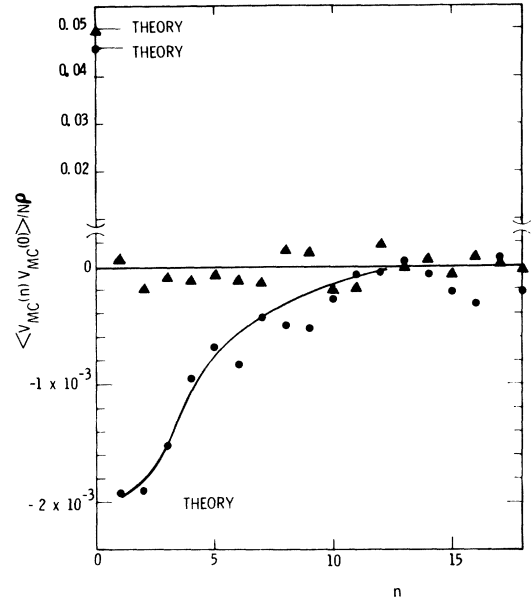


FIG. 6. Monte Carlo zero-field velocity correlation per particle vs Monte Carlo time interger  $n$ . Circles are for  $W_{AB}=0.1 W_{BA}$  ( $p_{AB}=0.02, p_{BA}=0.2$ ). Triangles are for  $W_{AB}=W_{BA}$  ( $p_{AB}=p_{BA}=0.05$ ). Both sets of data are for  $N\rho=100$  particles on 200 sites, average over 100 000 different thermal equilibrium initial conditions. Theoretical values from Eqs. (50) and (56) are indicated. Note the change in scale on the ordinate. The curve is meant as an aid to the eye only.

same order of magnitude. This may be seen by noting that  $\beta(0+)$  is of the order of  $W^2$  and it decays at a rate proportional to  $W$ . Thus  $|\int_0^\infty \beta(t) dt| \sim W^2/W = W$ , which is of the same order as  $\alpha$ . Here we have used  $W$  to stand for  $W_{AB}, W_{BA}$  or some linear combination of the two. Since the complete conductivity  $\sigma$  is less than  $\sigma_{MF}$  according to Eq. (42), it follows that  $\int_0^\infty \beta(t) dt$ , as well as  $\beta(0+)$ , is negative. In particular, since  $\sigma/\sigma_{MF} \rightarrow 0$  as  $n_A \rightarrow 1$  according to Eq. (42), we have  $\int_0^\infty \beta(t) dt = -\frac{1}{2}\alpha$  for  $n_A \rightarrow 1$ , in which limit  $\beta(0) \rightarrow 0$  and  $\alpha \rightarrow 2Na^2 W_{AB}$  for the half-filled lattice ( $n_A + n_B = 1$ ).

That  $\beta(t)$  should be negative is expected from the nature of the correlations. Since hops to occupied sites are disallowed, it is more probable for a particle to hop back to its previous location (change sign of velocity) which is left vacant than to hop forward to a site which may be occupied.

Figure 6 shows the Monte Carlo velocity correlation per particle both for  $W_{AB}=W_{BA}$  and for  $W_{AB}=0.1 W_{BA}$ . The discontinuity between  $n=0$  and  $n=1$  is clearly seen, and the values at  $n=0$  and  $n=1$  agree well with theory. The  $n \geq 1$  correlation function for  $W_{AB}=0.1 W_{BA}$  decays to one-half of its negative initial value in three Monte Carlo steps, which corresponds to  $W_{AB}t=0.06$  for the hopping probability used,  $p_{AB}=0.02$ . By comparison the

correlation  $\bar{\beta}(t)$  given in Fig. 3 of Ref. 6 decays to one-half of its positive initial value at  $W_{AB}t = 0.04$ , so  $\beta(t)$  and  $\bar{\beta}(t)$  have similar decays even though they are of opposite sign. The results for  $W_{AB} = W_{BA}$  are consistent with  $\beta(t) = 0$  to within statistical error. Although we have not proved that  $\beta(t) = 0$  for equivalent sites, we have shown that both  $\beta(0+)$  and  $\int_0^\infty \beta(t) dt$  are zero (the latter follows from  $\sigma = \sigma_{MF}$  for  $W_{AB} = W_{BA}$ ), and it seems reasonable to assume that the stochastic hopping equations are consistent with  $\beta(t) = 0$  for all times.

### V. DIFFUSION

Thus far it has been adequate to consider the site occupancies only and not keep track of distinguishable particles. In this section we examine the motion of a single particle and show that it does not diffuse in the normal sense but rather has a mean square displacement given by Eq. (3) at sufficiently high density  $\rho$ .

Before treating the distinguishable particles it is useful to establish results for the net displacement of all the particles

$$X(t) = \sum_{\alpha} [x_{\alpha}(t) - x_{\alpha}(0)], \quad (57)$$

where  $x_{\alpha}(t)$  is the position of the  $\alpha$ th particle at time  $t$  and we use the convention that Greek indices label particles and Roman ones label sites. In his classic paper<sup>7</sup> Kubo pointed out that

$$\langle X(t)^2 \rangle = 2 \int_0^t d\tau (t - \tau) \langle V(\tau)V(0) \rangle, \quad (58)$$

since  $dX/dt = V$  and thus

$$D = \frac{1}{2N_P} \lim_{t \rightarrow \infty} \frac{\langle X(t)^2 \rangle}{t} = \frac{1}{N_P} \int_0^\infty d\tau \langle V(\tau)V(0) \rangle. \quad (59)$$

Equations (59) and (25) may be combined to give a generalized definition of the Einstein-Nerst formula for  $N_P$  interacting particles, as noted in Ref. 7. We were able to calculate the conductivity in Sec. IV and thereby also determine  $D$  according to the above prescription. The fact that the drift velocity  $V_E$  is linear in the field  $E$  for  $E \rightarrow 0$  is sufficient to establish convergence of the quantities in Eq. (59), by virtue of the Kubo formula (25).

That  $X(t)$  involves site probabilities only stems from the relations

$$x_{\alpha}(t) = \sum_i x_i g_{i, \alpha}(t), \quad (60)$$

$$P_i(t) = \sum_{\alpha} g_{i, \alpha}(t), \quad (61)$$

and thus

$$\sum_{\alpha} x_{\alpha}(t) = \sum_i x_i P_i(t), \quad (62)$$

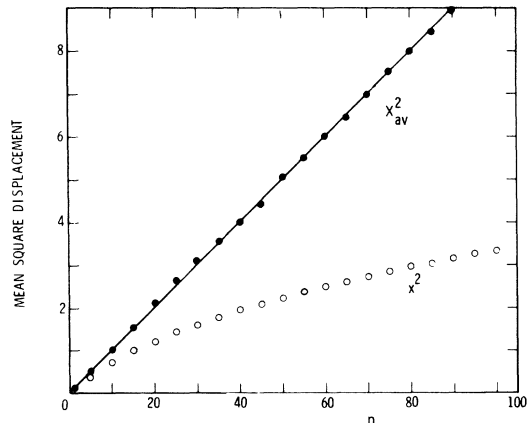


FIG. 7. Mean-square displacements vs Monte Carlo time  $n$ . Equivalent sites,  $p_{AB} = p_{BA} = 0.1$ ,  $\Delta = 0$ , 4000 particles on 8000 sites, average over 1600 different thermal-equilibrium initial conditions.

where  $g_{i, \alpha} = 1$  if particle  $\alpha$  is at site  $x_i$  and 0 otherwise. The motion of an individual distinguishable particle not only requires more than just site equations, its equations are more complex. This is most clearly seen for equivalent sites where the rate equations for a distinguishable particle are<sup>9</sup>

$$\begin{aligned} \langle \delta g_{i, \alpha}^* \rangle_{av} = & -p g_{i, \alpha} (2 - P_i - P_{i+1}) \\ & + p(1 - P_i)(g_{i+1, \alpha} + g_{i-1, \alpha}). \end{aligned} \quad (63)$$

Whereas in the site equations for  $p_{AB} = p_{BA} = p$  the nonlinear terms cancel, no such cancellation occurs here. One can therefore expect rather different behavior for properties connected with individual particle motion.

The mean-square displacement of a single particle, averaged over all the  $N_P$  particles and normalized to unit hopping distance, is

$$x^2 = a^{-2} N_P^{-1} \sum_{\alpha} \langle [x_{\alpha}(t) - x_{\alpha}(0)]^2 \rangle, \quad (64)$$

while the corresponding quantity for net displacement of all the particles  $X_{av}^2$  is given by taking the square of the sum in Eq. (57) rather than the sum of the squares as in (64):

$$X_{av}^2 = a^{-2} N_P^{-1} \left\langle \sum_{\alpha} x_{\alpha}(t) - x_{\alpha}(0) \right\rangle^2. \quad (65)$$

Computation of  $x^2$  involves keeping track of individual particles. This task is simplified in a linear chain since the particles always stay in order as long as double-site occupancy is forbidden. Details of the method may be found in the Appendix.

In the absence of correlations  $x^2 = X_{av}^2$ . Figure 7 shows Monte Carlo results for  $X_{av}^2$  and  $x^2$  vs  $t$ . Although  $X_{av}^2$  is linear in  $t$  with a slope in agreement with that predicted from the conductivity,  $x^2$  clearly

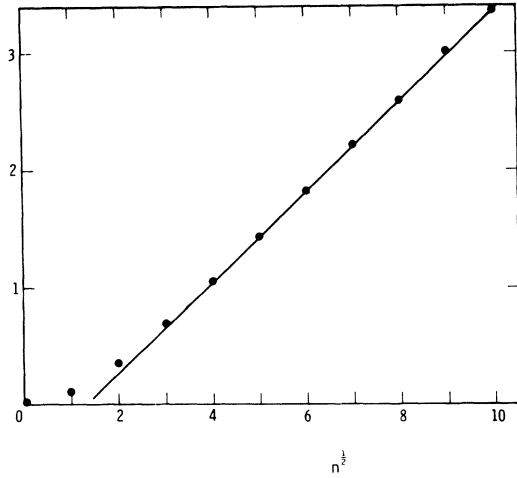


FIG. 8. Replot of average square single-particle displacement  $x^2$  in Fig. 7, now shown vs  $n^{1/2}$

is not. The single particle  $x^2$  is replotted versus  $t^{1/2}$  in Fig. 8 and a good straight-line fit is obtained for long times  $W_{AB}t \gtrsim 1$ .

We have not succeeded in obtaining a first-principles derivation of  $x^2 \propto t^{1/2}$  starting from the equations of motion, but feel that the result can be understood from the following semiquantitative agreement which relates a correlation length to density fluctuations. We start with the established diffusive behavior of  $X_{av}^2$ ,

$$\begin{aligned} X_{av}^2 &= a^{-2} N_P^{-1} \left\langle \sum_{\alpha, \beta} [x_{\alpha}(t) - x_{\alpha}(0)] [x_{\beta}(t) - x_{\beta}(0)] \right\rangle \\ &= 2Da^{-2}t. \end{aligned} \quad (66)$$

For equivalent sites in thermal equilibrium Eq. (66) may be rewritten

$$\begin{aligned} 2Da^{-2}t &= x^2 + a^{-2} \sum_{\beta \geq 1} \langle [x_0(t) - x_0(0)] [x_{\beta}(t) - x_{\beta}(0)] \rangle \\ &+ a^{-2} \sum_{\beta < -1} \langle [x_0(t) - x_0(0)] [x_{\beta}(t) - x_{\beta}(0)] \rangle. \end{aligned} \quad (67)$$

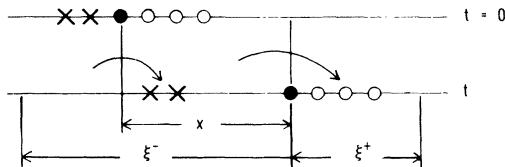


FIG. 9. Diagram accompanying argument surrounding Eqs. (68)–(76). Solid circle represents particle which moves a distance (normalized to unit nearest neighbor spacing)  $x$  in time  $t$ . Open circles are particles which get pushed ahead of it. Crosses are particles which move in to fill the void left behind.

Assume for the sake of argument that  $x_0(t) - x_0(0) > 0$  and that  $x_{\beta}(t) - x_{\beta}(0)$  is correlated with  $x_0(t) - x_0(0)$  over a distance  $\xi^+ a$  for  $\beta > 0$  and over a distance  $\xi^- a$  for  $\beta < 0$ . Then the number of particles involved in the two sums on the right-hand side of (67) are  $\rho\xi^+$  and  $\rho\xi^-$  so that

$$2Da^{-2}t = x^2 + x^2\rho(C^+\xi^+ + C^-\xi^-), \quad (68)$$

where  $C^+$  and  $C^-$  are constants of the order of unity and we have noted that  $a^{-2}\langle [x_0(t) - x_0(0)]^2 \rangle = x^2$ . If the dimensionless correlation lengths  $\xi^{\pm}$  were independent of time, Eq. (69) would simply reduce to  $x^2 = 2Da^{-2}ft$  with a correlation factor  $f = (1 + \rho C^+\xi^+ + \rho C^-\xi^-)^{-1}$  and the situation would be similar to that commonly treated in higher dimensions.<sup>4</sup> We argue, however, that  $\xi^{\pm}$  are themselves proportional to  $x^2$  for long times. Referring to Fig. 9, if the particle labeled zero moves a number of spaces  $x = [x_0(t) - x_0(0)]/a$  to the right in time  $t$  then it displaces on the average  $\rho x$  particles to the right.  $\xi^+$  is defined such that a particle at a distance (in units of  $a$ )  $\xi^+$  to the right of particle zero at time  $t$  is unaffected by this movement. In other words  $\xi^+$  is a region whose size can just “tolerate” the additional  $\rho x$  particles forced into it. The condition on toleration is assumed to be that  $\rho x$  corresponds to no more or no less than a thermal equilibrium fluctuation  $(\langle n^2 \rangle - \langle n \rangle^2)^{1/2}$  in the number of particles  $n$  contained in  $\xi^+$ . Since  $\langle n^2 \rangle - \langle n \rangle^2 = \langle n \rangle(1 - \rho)$  for a random distribution and  $\rho\xi^+ = \langle n \rangle$  is the mean number of particles contained in  $\xi^+$ , we make the relation

$$[\xi^+\rho(1 - \rho)]^{1/2} \approx \rho x. \quad (69)$$

If  $\xi^+$  were smaller than given by (69), the excess  $\rho x$  particles would represent more than a thermal fluctuation and there would be pressure to push more particles aside, increasing the correlation range. If  $\xi^+$  were greater than given by (69), the additional particles would constitute less than a normal statistical fluctuation and would not be noted.

A similar argument holds for  $\xi^-$ . If the region  $x$  is depleted, a number  $\rho(\xi^- - x)$  of particles will flow into it until the total region  $\xi^-$  has a number no less than that consistent with statistical fluctuations. Thus

$$\rho(\xi^- - x) \approx \rho\xi^- - [\rho(1 - \rho)\xi^-]^{1/2}. \quad (70)$$

Equations (69) and (70) show that  $\xi^+ = \xi^- = \xi$  and thence Eq. (68) becomes

$$2Da^{-2}t = x^2 + x^4\rho^2(1 - \rho)^{-1}(C^+ + C^-), \quad (71)$$

which establishes the dependence  $x^2 \propto t^{1/2}$  except at very low density.

Equivalent sites are implicitly assumed in the above argument. For the general case of inequiva-

lent sites the only difference is that the statistical fluctuation in the number of particles contained in  $\xi$  sites, half of which are *A* type and half of which are *B* type, is

$$\langle n^2 \rangle - \langle n \rangle^2 = \frac{1}{2} \xi [n_A(1 - n_A) + n_B(1 - n_B)], \quad (72)$$

where  $2\rho = n_A + n_B$ .

As long as the number of displaced particles is large, which is the case for long times, this number is still  $\rho x$ , so the same arguments go through with  $\xi^* = \xi$  given by

$$\xi = \rho x^2 / [1 - \rho - (n_A - n_B)^2 / 4\rho]. \quad (73)$$

For the half-filled lattice,  $\rho = \frac{1}{2}$ , Eq. (73) reduces to  $\xi = x^2 / 8n_A n_B$ .

The constants  $C^\pm$  are estimated as follows, where reference to Fig. 9 is advised. Consider first the summation

$$a^{-2} \sum_{\beta \geq 1} \langle [x_0(t) - x_0(0)][x_\beta(t) - x_\beta(0)] \rangle = x \sum_{\beta=1}^{\rho(\xi+x)} \frac{x_\beta(t) - x_\beta(0)}{a}, \quad (74)$$

where  $x_\beta(t)$  is calculated under the premise that  $\rho(x + \xi)$  particles are distributed over the distance  $\xi a$  with  $\beta=0$  at  $x$ , and we assume that  $x$  and  $\xi$  are sufficiently large that the region contains an equal number of *A* and *B* sites for the case of inequivalent sites.

Assume that the  $\rho(\xi + x)$  particles are equally dis-

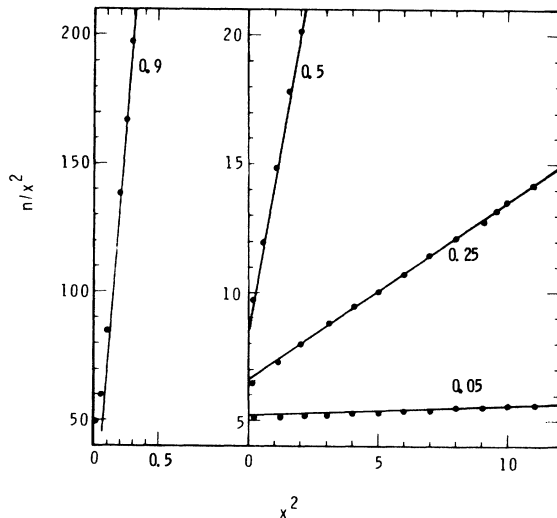


FIG. 10. Plots of  $n/x^2$  vs  $x^2$  as suggested by Eq. (76) for various particle densities  $\rho$  shown by numbers on figure. Data for  $\rho \leq 0.5$  are for runs with 8000 sites; for  $\rho = 0.9$  number of sites is 4000. All runs had  $p_{AB} = p_{BA} = 0.105$ ,  $\Delta = 0$ , and show an average over 200 different thermal-equilibrium initial conditions at each  $\rho$  value.

tributed over the space between  $x$  and  $x + \xi$  at  $t$  and over the space between 0 and  $x + \xi$  at  $t = 0$ . Then the sum reduces to

$$\rho(\xi + x) \left[ \frac{1}{2}(x + \xi + x) - \frac{1}{2}(x + \xi) \right] = \frac{1}{2} \rho x (\xi + x),$$

since it is just the number of particles times their average displacement. The argument applies equally well for inequivalent sites as long as we understand that  $x$  and  $\xi$  are sufficiently large that they contain a number of *AB* units and the mean position can be taken as midway between an *A* and its neighboring *B* site.

Similarly, the sum for  $\beta \leq -1$  is computed by assuming that the distribution of  $\rho(\xi - x)$  particles is between  $-(\xi - x)$  and 0 at  $t = 0$  and between  $-\xi$  and 0 at  $t$ , so

$$\sum_{\beta \leq -1} \frac{x_\beta(t) - x_\beta(0)}{a} = \rho(\xi - x) \left[ -\frac{1}{2}\xi - (-\frac{1}{2})(\xi - x) \right] = \frac{1}{2} \rho x (\xi - x). \quad (75)$$

Combining the two results we see that  $C^+ + C^- = 1$  so that Eqs. (71) and (73) reduce in the general case to

$$2Da^{-2}t = x^2 + x^4\rho^2 [1 - \rho - (n_A - n_B)^2 / 4\rho]^{-1}. \quad (76)$$

Equation (76) suggests a manner of plotting and predicts a density and occupation number dependence.

A plot of  $t/x^2$  vs  $x^2$  should give a straight line whose intercept is  $a^2/2D$  and whose slope-to-intercept ratio is  $\rho^2(1 - \rho)^{-1}$  for equivalent sites. Figure 10 presents such plots for several values of  $\rho$  with  $W_{AB} = W_{BA} = W$ . There is some curvature near  $x^2 = 0$  but straight-line portions are clearly seen. The  $t = 0$  values of the curves are compared with the theoretical value  $a^2/2D = [2W(1 - \rho)]^{-1}$  in Table I and excellent agreement is found up to the highest density studied,  $\rho = 0.9$ . The ratio  $S/L$  of the slope of the straight-line portion to the  $t = 0$  value is plotted versus  $\rho^2(1 - \rho)^{-1}$  in Fig. 11. A good straight line is

TABLE I. Comparison between theoretical diffusion coefficient  $D$  and  $t \rightarrow 0$  limit of  $Wt/x^2$  for  $W_{AB} = W_{BA} = W$  obtained from Fig. 11. (Conversion is made from  $n/x^2$  to  $Wt/x^2$  by using  $p_n = Wt$ , where  $p = 0.105$  for the curves in Fig. 11.)

$\rho$	$\frac{a^2 W}{2D}$	$\lim_{t \rightarrow 0} \left( \frac{Wt}{x^2} \right)$
0.05	0.53	0.54
0.167	0.60	0.59
0.25	0.67	0.66
0.434	0.88	0.87
0.5	1.00	0.95
0.75	2.00	2.00
0.9	5.00	5.14

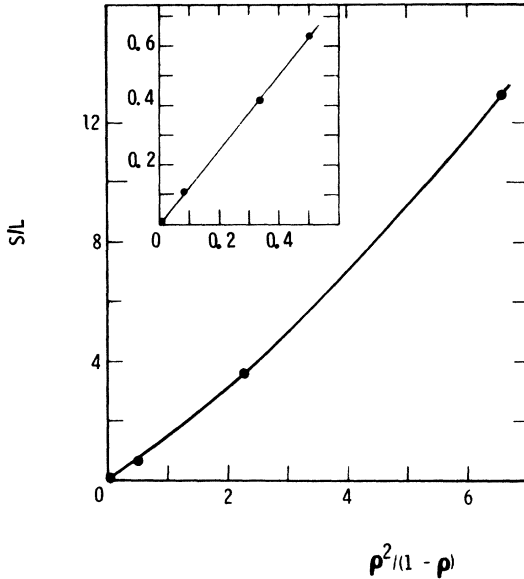


FIG. 11. Slope  $S$  of straight-line portion of curves in Fig. 10 divided by the  $x^2 \rightarrow 0$  limit  $L$  of the curve vs  $\rho^2/(1-\rho)$ . Inset gives expanded view of  $\rho \leq 0.5$  region.

obtained for  $\rho \leq 0.5$  whose slope of 1.25 agrees closely with the estimate of unity ( $C^+ + C^- = 1$ ), but there is a pronounced upward curvature for the higher densities.

We have also plotted (not shown)  $t/x^2$  vs  $x^2$  for  $W_{AB} = 0.1 W_{BA}$ . Here we neither expect nor find a straight line near  $t=0$  since the relation  $X_{av}^2 = 2Dt$  holds only for long times when  $W_{AB} \neq W_{BA}$ , i.e., one has to wait for the  $\beta(t)$  part of the velocity correlation to decay to zero. We do find straight-line behavior for  $W_{AB} t \geq 20$  with a slope 19% less than predicted by Eq. (76).

In view of the relative crudeness of the model, we regard the overall agreement as quite satisfactory and in support of the basic physical picture which relates the size of the correlated region to one in which the extra number of particles entering just corresponds to an average thermal fluctuation. The key to this correlation is the fact that in the restricted 1D system a particle cannot move without forcing other particles to move ahead of it. For this reason, the effect  $x^2 \propto t^{1/2}$  is likely to occur only in 1D.

It is worthwhile to note that the agreement in Table I shows that there is no time-independent correlation effect, i.e., the distances  $\xi^\pm$  in Eq. (68) go to zero as  $t \rightarrow 0$  so that the correlations can in no way be accounted for by a constant correlation factor.

We mention that a similar dependence  $c^2 \propto t^{1/2}$  has been derived for the mean-square displacement  $c^2$  of a defect of a polymer chain.<sup>10</sup> However, the

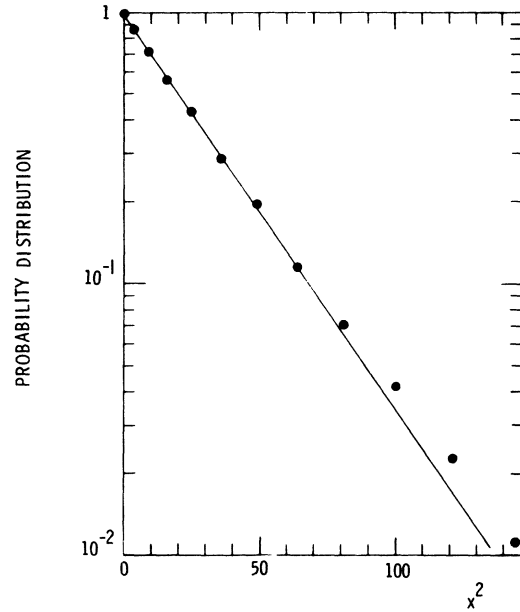


FIG. 12. Probability distribution  $g(x,t)/g(0,t)$  at  $Wt = 200$  vs  $x^2$ . Data are for  $W_{AB} = W_{BA} = W$  ( $p_{AB} = p_{BA} = 0.1$ ),  $\Delta = 0$ , 4000 particles on 8000 sites, average over 40 different initial thermal-equilibrium conditions.

mechanism appears to be quite different there and, in fact, the defects are assumed to move independently.

Figure 12 gives the distribution  $g(x,t)$  which is the average probability that a particle has traveled a distance  $x$  in the time  $t$ . For the long time  $Wt = 200$ ,  $g(x,t)$  is nearly Gaussian for two decades. Since the mean square displacement is known from the above, we can then assert that the normalized probability distribution has the form

$$g(x,t) = (2\pi)^{-1/2} (bt)^{-1/4} \exp[-x^2/2(bt)^{1/2}] \quad (77)$$

for long times, where

$$b = \frac{2(1.25)D(1-\rho)}{\rho^2} = \frac{2.5Wa^2(1-\rho)^2}{\rho^2}, \quad (78)$$

where 1.25 is the "experimental" (computed) factor deduced from Fig. 11 and equivalent sites  $W_{AB} = W_{BA} = W$  are assumed. The above should be reasonably accurate for  $\rho \leq \frac{1}{2}$ , but deviations can be expected at higher densities in view of the departure from theory seen in Fig. 11.

## VI. SUMMARY AND DISCUSSION

This paper has considered hopping on a linear chain in which no two particles can occupy the same site, but the particles are otherwise noninteracting. The general case of two inequivalent sites per unit cell was studied. Classical transition rate equations were set up and solved both by Monte

Carlo simulation and, where possible, by analytical techniques.

The main results are as follows. If a "mean-field" equation or solution is defined as one for which the only effect of forbidden hops to occupied sites is to reduce a transition rate by the factor  $1 - n_{A,B}$  for hops to  $A, B$  sites, where  $n_{A,B}$  is the average occupation number, then the bulk conductivity and diffusion obey mean-field equations for the special case of equivalent sites  $n_A = n_B$ . However, there is a major departure from mean-field behavior for inequivalent sites. The activation energy for conductivity is increased from its mean-field value of  $\Delta_A$  to  $\Delta_A + \frac{1}{2}(\Delta_A - \Delta_B)$  if  $\Delta_A$  and  $\Delta_B$  are barrier heights for jumping out of deep  $A$  and shallow  $B$  sites, respectively, and the lattice is half-filled with  $\exp(\Delta_A/k_B T) \gg \exp(\Delta_B/k_B T) \gg 1$ . Conductivity and bulk diffusion, which can be described solely by site occupancies, are still connected by the Einstein-Nernst relation for the inequivalent site problem so that anything said in general about one holds for the other as well.

Mean-field theory breaks down completely for the motion of a single distinguishable particle. The mean-square displacement  $x^2$  obeys  $x^2 = 2(bt)^{1/2}$  rather than the diffusive (and mean-field) dependence  $x^2 = 2Dt$  upon time  $t$ . This behavior was explained by a semiquantitative argument which equated the number of particles which must get pushed into a region of correlation size  $\xi$  when a particle moves the distance  $x$  to the rms statistical fluctuation in the number particles contained in  $\xi$ . The argument predicted a density and occupation number dependence of  $b$  which were verified by the Monte Carlo results.

The relation between stochastic hopping equations used here and the nonlinear rate equations used in Ref. 6 was explored. Only in the case of equivalent sites, where the nonlinearities cancel out, do the two methods coincide. In general the site autocorrelation decays more slowly in the stochastic model (Fig. 2). There is a much more significant qualitative difference for the velocity correlation function which decays smoothly to zero without oscillation in Ref. 6 but which, we argued, becomes negative for times greater than, but not including, zero. Careful examination of the probabilistic equations showed that the velocity correlation has a  $\delta$  function behavior at  $t=0$  neglected in Ref. 6 but which in fact just reproduces the mean-field conductivity in the Kubo formalism.

Let us examine some of the possible consequences of this work for real systems. Much of the attention will focus on the superionic conductor  $\beta$ -eucryptite ( $\text{LiAlSiO}_4$  with the  $\beta$ -quartz structure). It has a large ionic conductivity<sup>11</sup> which has recently been confirmed in single crystals,<sup>12</sup> and its

structure<sup>13</sup> and anisotropy of dielectric constant<sup>14</sup> suggest that the conduction takes place dominantly along 1D channels. Below about 460 °C the structure further suggests inequivalent sites with  $n_B \ll n_A \approx 1$ . We write the "hard-hop"  $A \rightarrow B$  transition rate as  $W_{AB} = \nu_0 \exp(-\Delta_A/k_B T)$ , where  $\Delta_A$  is an appropriate activation energy and  $\nu_0$  is usually identified as an attempt frequency which is of the order of an optical-phonon frequency. (The number of vacancies in  $\beta$ -eucryptite is temperature independent corresponding to  $\rho = \frac{1}{2}$ . Thus questions of vacancy formation do not enter into consideration of  $\nu_0$ .) Raman scattering<sup>15</sup> has shown a line at 160  $\text{cm}^{-1}$  which was identified with the attempt frequency. This gives  $\nu_0 = 4.8 \times 10^{12} \text{ sec}^{-1}$ , a sensible optical-phonon value. The thermally activated single-crystal conductivity<sup>12</sup>  $\sigma = \sigma_0 \exp(-\Delta'/k_B T)$ , however, has a preexponential  $\sigma_0 = 3 \times 10^4 \Omega^{-1} \text{ cm}^{-1}$  at 400 °C. If mean-field theory holds, then  $\Delta' = \Delta_A$  and  $\sigma_0 = Ne^2 a^2 \nu_0 / \Omega k_B T$ , which converts to  $\nu_0 \approx 10^{15} \text{ sec}^{-1}$  for the  $\beta$ -eucryptite lattice. There is thus a discrepancy of a factor of 200 between the Raman and mean-field conductivity values of the attempt frequency. This may be partially resolved by noting that the correct expression from Eqs. (35) and (43) would give  $\Delta' = \frac{3}{2}\Delta_A$  and  $\nu_0$  (conductivity)  $= 2\nu_0^{3/2} / W_{BA}^{1/2}$  for  $W_{BA} \gg W_{AB}$  if we assume now that the rate  $W_{BA}$  which, for example, could occur by tunneling without the need for thermal activation is only weakly temperature dependent compared with the thermally activated  $W_{AB}$ . In the above  $\nu_0$  (conductivity) is the attempt frequency which would be inferred from analyzing the experimental conductivity with the mean-field formula. Since we expect  $W_{BA} \ll \nu_0$  as long as  $B$  is a stable equilibrium site, the effect is in the right direction. The single-crystal conductivity has an activation energy<sup>12</sup>  $\Delta' = 0.83 \text{ eV}$ , which would give  $\nu_0/W_{AB} = 1.4 \times 10^4$  ( $\Delta_A = \frac{2}{3}\Delta'$ ) at 400 °C, so it is possible to satisfy both  $W_{BA} \ll \nu_0$  and  $W_{BA} \gg W_{AB}$ . Clearly it would be desirable to have a Raman measurement of the activation energy to see if the prediction  $\Delta_A = \frac{2}{3}\Delta'$  is borne out.

NMR studies in  $\beta$ -eucryptite have revealed further anomalies which are discussed in separate publications<sup>5,8</sup> that make use of some of the results presented here. Nuclear-relaxation times are governed by Fourier components of time-correlation functions at the NMR frequency  $\omega$ . Both site and distinguishable particle correlations are involved. For the latter we have seen that the characteristic decay rate  $b$  if of the order of  $Dn_A n_B \sim W_{AB}(W_{AB}/W_{BA})$  for long times and  $\rho = \frac{1}{2}$  with  $n_B \ll n_A \approx 1$  [see Eqs. (43) and (76)]. Thus the NMR correlation time can have an even greater enhancement of the activation energy, by another factor of 1.5 if the temperature dependence of  $W_{BA}$  is ne-

glected, than the conductivity has. This leads to a very slow long time decay at the lower temperatures, a fact which is utilized in Refs. 5 and 8.

It is well known that the slow decay of correlations in 1D can produce anomalous magnetic-resonance line shapes, linewidths, and frequency-dependent relaxation times.<sup>16</sup> This is true even for mean-field behavior where the correlations decay as  $t^{-1/2}$ . The effect is all the more pronounced here where the slower  $t^{-1/4}$  decay is predicted by Eq. (77). de Gennes<sup>10</sup> has previously noted that such decay leads to an  $\omega^{-3/4}$  dependence of the longitudinal relaxation rate  $T_1^{-1}$  for  $\omega \rightarrow 0$ , whereas the behavior is  $\omega^{-1/2}$  for a  $t^{-1/2}$  dependence. In order to observe this, however, the frequency must be in the range  $t_0^{-1} < \omega < b$ , where  $t_0$  is a characteristic time for interchannel hopping which cuts off the slow decay and  $b$  is the previously introduced slow decay rate. If  $\omega < t_0^{-1}$  the rate  $T_1^{-1}$  levels off at a large frequency-independent value, and if  $\omega > b$  only the short-time part of the decay contributes to  $T_1$ . Thus one must choose his frequency and temperature range carefully, and it is unlikely that the conditions have been satisfied in previous work on  $\beta$ -eucryptite.

The 1D hopping model with equivalent sites has also been applied to NMR studies<sup>9</sup> of organic charge transfer salts based on tetracyanoquinodimethane (TCNQ). A mean-field solution was used whereby it was predicted that the correlations decay at a rate proportional to  $1 - \rho$ . The NMR relaxation rate for interaction with a density  $\rho$  of hopping electrons would then have a density dependence given by

$$\left(\frac{1}{T_1}\right)_{\text{MF}} \propto \rho \int_0^{t_0} (Dt)^{-1/2} dt \sim \rho(1 - \rho)^{-1/2} t_0^{1/2}$$

in the  $\omega \rightarrow 0$  limit for the mean-field value with a cutoff time  $t_0$ . The corresponding prediction here is

$$\frac{1}{T_1} \propto \rho \int_0^{t_0} (bt)^{-1/4} dt \sim \rho^{3/2}(1 - \rho)^{-1/2} t_0^{3/4},$$

with the dependence of  $b$  upon  $\rho$  given by Eq. (78). In Ref. 9 it was tacitly assumed that  $t_0^{-1} \propto 1 - \rho$  and good agreement was thereby obtained with the  $\rho$  dependence of  $T_1$  for three TCNQ salts. Since  $t_0$ , in general, reflects hopping to a chain with *different* density (except for  $\rho = \frac{1}{2}$ ), the relation  $t_0^{-1} \propto 1 - \rho$  may not be justified even in mean-field theory. This combined with what we feel is the inadequacy of MF may make the agreement found in Ref. 9 somewhat fortuitous.

Repulsion between carriers on different sites, which can be important in the ionic conductors where there is less screening than in electronic ones, has been neglected here.<sup>17</sup> It can lead to co-

operative effects which may play a role in the apparent order-disorder transition in  $\beta$ -eucryptite.<sup>5,14</sup> However, the same-site repulsion (assumed to be infinite here) has been shown by itself to lead to novel effects which suggest new experiments and reinterpretation of some old ones.

#### ACKNOWLEDGMENTS

I have benefited from discussions with W. Camp, D. Emin, and D. Huber. Helpful advice on computing techniques was given by J. Van Dyke. Reference 10 was called to my attention by P. Pincus.

#### APPENDIX: DETAILS OF MONTE CARLO CALCULATION

We describe how initial conditions are chosen, how the steps in Eq. (7) are carried out in practice, and how particles are kept track of when distinguishable single-particle properties are computed.

Initial conditions corresponding to thermal equilibrium are of most interest since they are needed for calculations of the various thermal-equilibrium time correlation functions. A common practice in Monte Carlo calculations<sup>18</sup> is to start with some ordered configurations, say all  $A$  sites occupied and all  $B$  sites unoccupied for  $\rho = \frac{1}{2}$ , and let the system come to equilibrium through application of the hopping equations over a large number of Monte Carlo steps  $n$ . In fact the aim often is to find just what the equilibrium state is. Here we know (Sec. III) the static equilibrium properties, and we found that a great deal of computer time was expended in reaching thermal equilibrium from an ordered state. Thus initial conditions were chosen as follows. For a given  $\rho$  and ratio  $p_{AB}/p_{BA} = W_{AB}/W_{BA}$  the thermal-equilibrium state is assumed to be one in which there are  $\frac{1}{2}Nn_A$  ( $\frac{1}{2}Nn_B$ ) particles distributed randomly on  $A$  ( $B$ ) sites where  $n_{A,B}$  are given in Sec. III. This state is obtained by generating a random sequence of the odd numbers  $1, 3, \dots, N-1$  and then saying that the first  $N_A = \frac{1}{2}Nn_A$  of these numbers are sites for which  $P_{iA} = 1$  (occupied) and the next  $\frac{1}{2}N(1 - n_A)$  have  $P_{iA} = 0$ . The procedure is repeated with the even numbers  $2, 4, \dots, N$  to put  $N_B = \frac{1}{2}Nn_B$  particles at random on the  $\frac{1}{2}NB$  sites. Each run starts with a different initial condition corresponding to the different random sequences.

The hopping Eq. (7) is applied at each "time" interval  $n$  by setting each  $P_i = \bar{P}_i$ , where  $\bar{P}_i$  is the value after all hops at the previous time  $n-1$  are accounted for. The sites  $i=1$  to  $N$  are then examined. If  $\bar{P}_i = 0$ , the site is skipped over. If  $\bar{P}_i = 1$  the site is again skipped over if  $\bar{P}_{i+1} = \bar{P}_{i-1} = 1$  since there are no neighboring vacancies into which the particle at  $i$  can hop. If  $\bar{P}_i = 1$ ,  $\bar{P}_{i+1} = 1$ , and  $\bar{P}_{i-1} = 0$ , the random number  $R$  is called. If  $R$  is greater than  $p_{i, i-1}$  the site is skipped over, but if  $R \leq p_{i, i-1}$ ,

a jump occurs and we make the changes  $P_i \rightarrow P_i - 1$ ,  $P_{i-1} \rightarrow P_{i-1} + 1$  and set the array element  $JL(i) = 1$  which indicates that the particle which was at site  $i$  jumped to the left. A similar procedure is followed for  $\bar{P}_i = 1$ ,  $\bar{P}_{i-1} = 1$ ,  $\bar{P}_{i+1} = 0$ . If  $\bar{P}_i = 1$  and both  $\bar{P}_{i+1}$  and  $\bar{P}_{i-1}$  are zero, a jump occurs if  $R \leq p_{i,i+1} + p_{i,i-1}$ , and a second random number  $R'$  is called to determine whether the jump was to the left or to the right. If  $R' \leq q$  the jump is to the right and thus  $P_i \rightarrow P_i - 1$ ,  $P_{i+1} \rightarrow P_{i+1} + 1$ ,  $JR(i) = 1$ ; and if  $R' \geq q$  the jump is to the left with corresponding changes in the  $P$ 's and  $JL(i) = 1$ . Here we define

$$q = (p_{i,i+1}/p_{i,i-1}) / (1 + p_{i,i+1}/p_{i,i-1}), \quad (A1)$$

so that the probabilities of  $i \rightarrow i + 1$  and  $i \rightarrow i - 1$  jumps are in the ratio  $p_{i,i+1}/p_{i,i-1}$  when both  $i + 1$  and  $i - 1$  are unoccupied. Note that  $q = \frac{1}{2}$  in the absence of a field.

The above procedure is carried out for each of the  $N$  sites in the fixed sequence  $i = 1, 2, \dots, N$ . By using  $\bar{P}_i$  rather than  $P_i$  at each site we avoid having to call the sites in a random sequence at each time  $n$ . That is, even if a jump occurred from  $i$  to  $i + 1$  at  $n$ , we still take  $i + 1$  as unoccupied when it and  $i + 2$  are examined at time  $n$ . Thus the order in which the sites are called does not prejudice the results. Periodic boundary conditions are assumed by taking  $i + 1 = 1$  for  $i = N$  and  $i - 1 = N$  for  $i = 1$ .

The method does, however, create the problem that, at the end of the sequencing, some sites can be doubly occupied. If, for example  $\bar{P}_{i+1} = \bar{P}_{i-1} = 1$ ,  $\bar{P}_i = 0$  and  $JL(i + 1) = JR(i - 1) = 1$  both the particles at  $i + 1$  and  $i - 1$  will jump into  $i$ , giving  $P_i = 2$ . (When a jump occurs to  $i$  we set  $P_i \rightarrow P_i + 1$  rather than  $P_i = 1$  or  $P_i = \bar{P}_i + 1$  so that this effect can be detected and corrected for.) Correction is made by examining each of the sites for double occupancy. If  $P_i \neq 2$ , the site is skipped over. If  $P_i = 2$ , the random number  $R'$  is called. If  $R' \leq q$  we say that the hop to the right is allowed and the one to the left dis-

allowed and thus make the changes  $P_i \rightarrow P_i - 1$ ,  $P_{i+1} \rightarrow P_{i+1} + 1$ ,  $JL(i + 1) = 0$ . Similarly, if  $R' > q$ ,  $P_i \rightarrow P_i - 1$ ,  $P_{i-1} \rightarrow P_{i-1} + 1$ ,  $JR(i - 1) = 0$ . Note that, for example, sending a particle back to  $i + 1$  does not create the possibility of  $i + 1$  now being doubly occupied. This is because if an  $i + 1 \rightarrow i$  jump occurred, we had to have  $\bar{P}_{i+1} = 1$  which prevented an  $i + 2 \rightarrow i + 1$  jump.

After all sites have been examined for possible hopping and the corrections for double occupancy have been made, we set  $\bar{P}_i = P_i$ ,  $JL(i) = JR(i) = 0$  and repeat the procedure for the next time interval  $n + 1$ .

Since impenetrable particles on a linear chain cannot get out of order, once the particle labeled  $\alpha = 1$  is located the location of all others follows simply by examining site occupancy. The array  $L(\alpha)$  is defined by  $L(\alpha) = i_\alpha$  where  $i_\alpha$  is the site at which the  $\alpha$ th particle resides. If  $L(1) = i_1$ , it then follows that  $L(2) = i_1 + s_1 = i_2$ ,  $L(3) = i_2 + s_2$ , etc., where  $s_\alpha$  is the number of sites one has to move to the right of  $i_\alpha$  to find an occupied site, i.e.,  $P_i = 0$  for  $i_\alpha < i < i_\alpha + s_\alpha$ ,  $P_i = 1$  for  $i = i_\alpha + s_\alpha$ . We therefore only need to keep track of particle number 1. It is initially located by the convention that it is at the first occupied odd numbered  $A$  site. If  $L(1) = \bar{i}$  after time  $n - 1$ , it is given after time  $n$  according to

$$L(1) = \begin{cases} \bar{i} & \text{if } JL(\bar{i}) = JR(\bar{i}) = 0, \\ \bar{i} + 1 & \text{if } JR(\bar{i}) = 1, \\ \bar{i} - 1 & \text{if } JL(\bar{i}) = 1. \end{cases}$$

The computations were carried out on the CDC 7600 computer at Sandia. A typical set of runs consisted of 4000 particles with the number of time intervals  $n = 1000$  and the number of runs with different initial conditions equal to 40. It would take about 1 h of central processor time to complete the  $4000 \times 100 \times 40 = 1.6 \times 10^7$  individual Monte Carlo steps, or about 20  $\mu$ sec per step.

\*Work supported by the U. S. ERDA under Contract No. AT(29-1)789.

<sup>1</sup>For a general description, see W. van Gool in *Fast Ion Transport in Solids*, edited by W. van Gool (North-Holland, Amsterdam, 1973), pp. 201-215.

<sup>2</sup>See, for example, A. J. Heeger, A. F. Garito, and L. V. Interrante, in *Low-Dimensional Cooperative Phenomena*, edited by H. J. Keller (Plenum, New York, 1975), pp. 89-124 and 299-314.

<sup>3</sup>Contained in most introductory texts on solid state physics, such as C. Kittel, *Introduction to Solid State Physics*, 2nd ed. (Wiley, New York, 1956), p. 368.

<sup>4</sup>See, for example, A. D. LeClaire, in Ref. 1, pp. 51-59.

<sup>5</sup>D. M. Follstaedt and P. M. Richards, *Phys. Rev. Lett.* **37**, 1571 (1976).

<sup>6</sup>D. L. Huber, *Phys. Rev. B* **15**, 533 (1977).

<sup>7</sup>R. Kubo, *J. Phys. Soc. Jpn.* **12**, 570 (1957).

<sup>8</sup>D. M. Follstaedt and P. M. Richards (unpublished).

<sup>9</sup>M. A. Butler, L. R. Walker, and Z. G. Soos, *J. Chem. Phys.* **64**, 3592 (1976).

<sup>10</sup>P. G. de Gennes, *J. Chem. Phys.* **55**, 572 (1971).

<sup>11</sup>R. T. Johnson, B. Morosin, M. L. Knotek, and R. M. Biefeld, *J. Electrochem. Soc.* **123**, 680 (1976).

<sup>12</sup>R. T. Johnson (private communication).

<sup>13</sup>H. Schultz and V. Tscherry, *Acta Crystallogr. B* **28**, 2168 (1972); V. Tscherry, H. Schultz, and F. Laves, *Z. Kristallogr.* **135**, 161 (1972).

<sup>14</sup>H. Böhm, *Phys. Status Solidi A* **30**, 531 (1975).

<sup>15</sup>B. Morosin and P. Peercy, *Phys. Lett. A* **53**, 147 (1975).



<sup>16</sup>For reviews, see D. W. Hone and P. W. Richards, *Ann. Rev. Materials Sci.* 4, 337 (1974); P. M. Richards, Ref. 2, pp. 147–169; P. M. Richards, in *Proceedings of International School of Physics, Enrico, Fermi, Course LIX*, edited by K. A. Muller (North-Holland,

Amsterdam, 1976), pp. 539–606.

<sup>17</sup>Kikuchi (in Ref. 1, p. 555) has treated 1D conductivity including nearest-neighbor repulsion, but only in the “mean-field” sense as defined here.

<sup>18</sup>K. Binder, *Adv. Phys.* 23, 917 (1974).